# Supplementary Figure 1

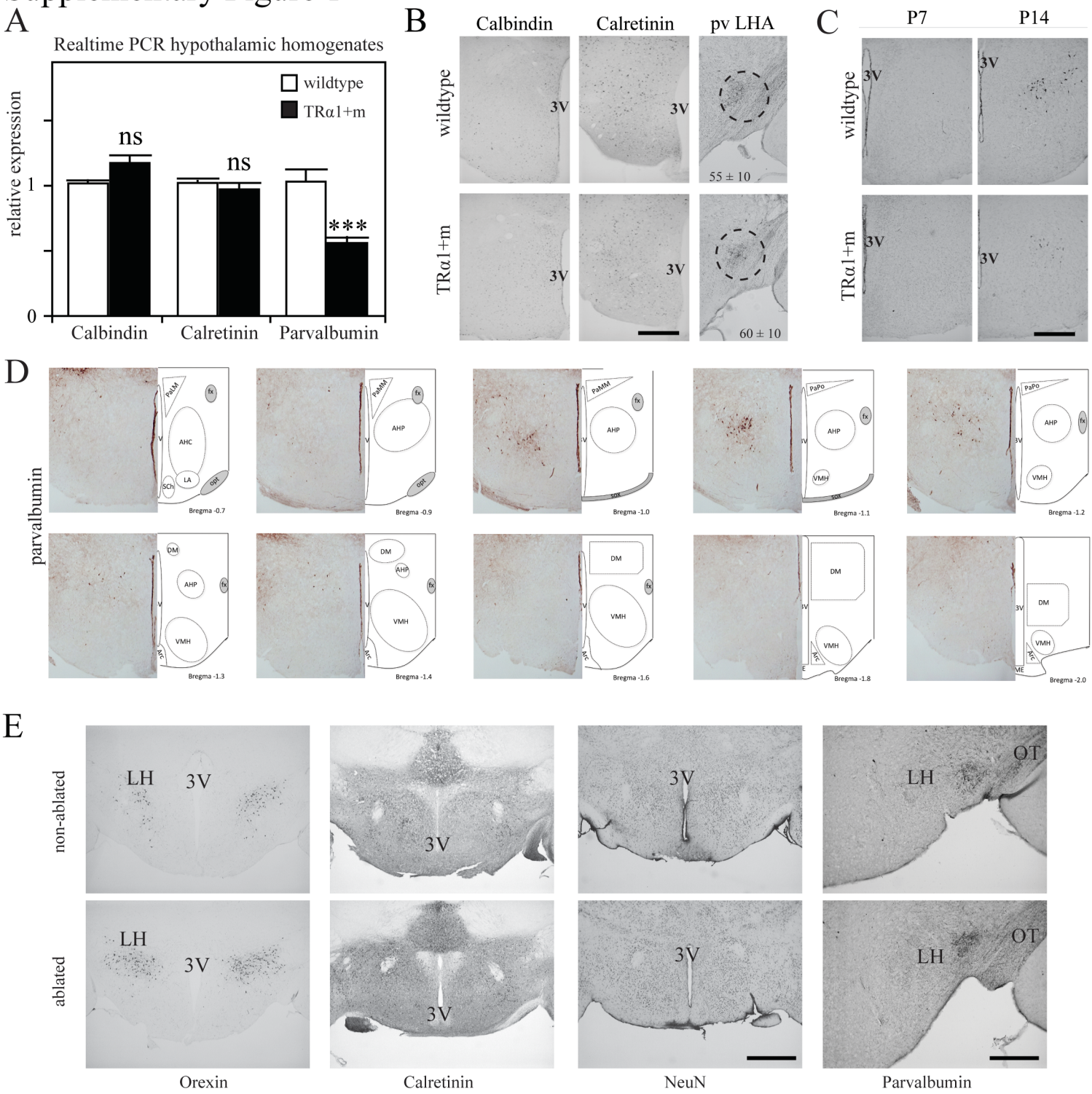


Supplementary Figure 1: A. Realtime qPCR in hypothalamic homogenates of wildtype mice and TRα1+m mice (***:p<0.001, n=5). B. Immunohistochemistry in hypothalamic sections of wildtype and TRα1+m mice for calbindin and calretinin (3V: 3rd ventricle, scale bar 250µm), as well as for parvalbumin in the lateral hypothalamic area (circle, raw count at the bottom of each picture, n=3 per group, p=0.55). C. Immunohistochemistry for parvalbumin in hypothalamic sections of wildtype and TRα1+m mice at postnatal day 7 (P7) and 14 (P14) (3V: 3rd ventricle, scale bar 250µm). D. Immunohistochemistry for parvalbumin in consecutive hypothalamic sections of wildtype mice with a corresponding scheme of the hypothalamic nuclei and the respective Bregma coordinates. Sections rostral and caudal to the area presented did not show any pv+ cells in the hypothalamus. Arc: arcuate nucleus; AH: anterior hypothalamus; DM: dorsomedial hypothalamus; fx: fornix; ME: median emminence; opt: optic tract; Pa: paraventricular nucleus; VMH: ventromedial hypothalamus; 3V: 3rd ventricle. E. Immunohistochemistry for orexin, calretinin and NeuN in hypothalamus of mice with AAV induced pv ablation (lower panel) and controls (upper panel, scale bar 500µm). Right panel shows a close-up of the recently described nucleus of pvneurons in the lateral hypothalamus, which is not affected by the AAV injection into the AHA (scale bar 200µm). 3V: 3rd ventricle; LH: lateral hypothalamus; OT: optic tract.

# Supplementary Figure 2

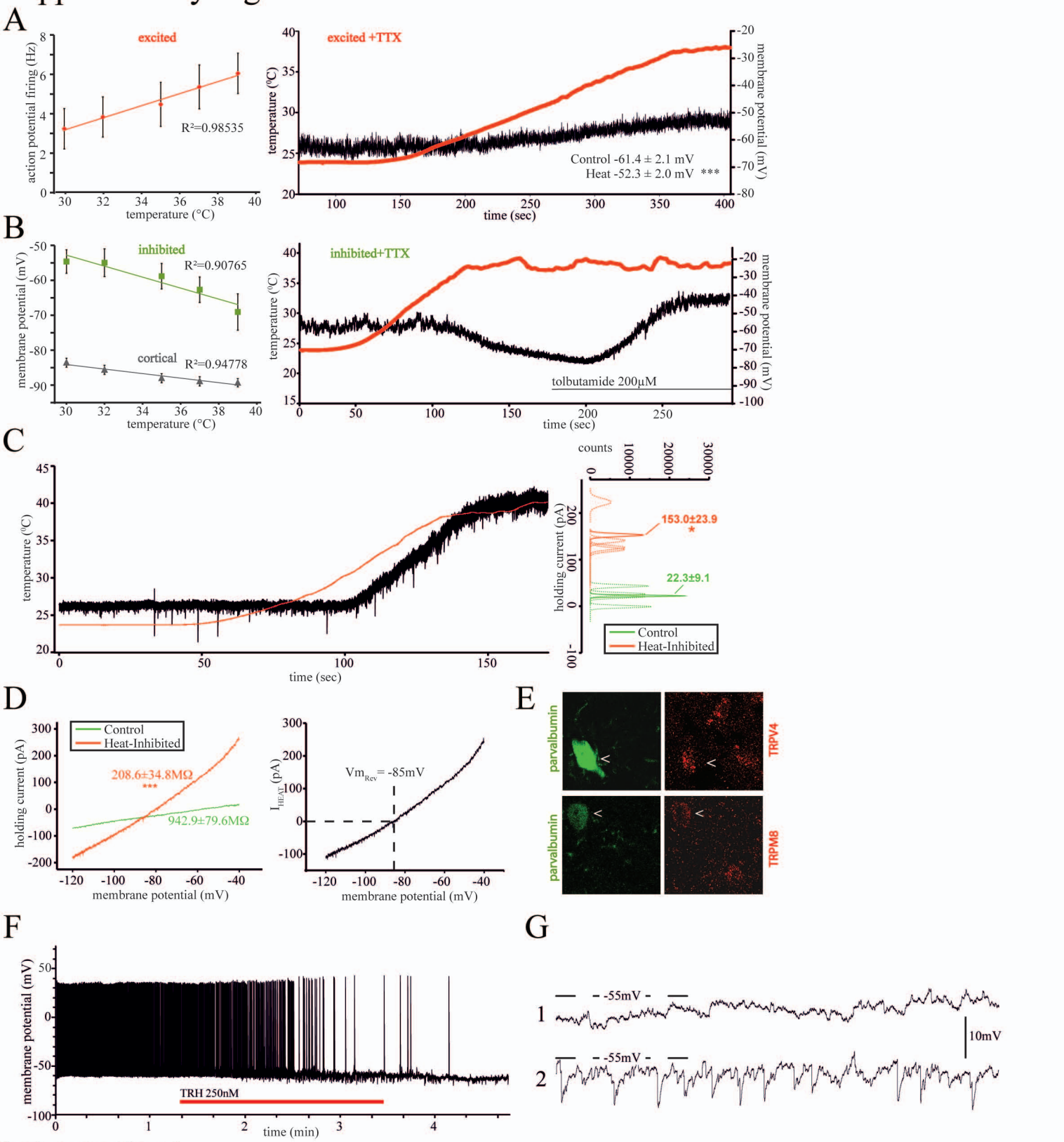


Supplementary Figure 2:

A. Temperature dependency of the firing frequency in heat excited parvalbuminergic neurons from the anterior hypothalamus (left panel) with current clamp recording in the presence of TTX. Ramping of temperature to 40°C results in depolarization by 9.1mV (n=5, p>0.005). B. Membrane potential in heat inhibited parvalbuminergic neurons from the anterior hypothalamus (left panel, slope -1,57) with cortical pv neurons as negative control (slope -0,65, note that the action potential firing ceases upon heat, thus temperature dependency of the firing frequency cannot be calculated for the physiological range) and current clamp recording in the presence of TTX. Ramping of temperature to 40°C results in a pronounced hyperpolarization that is reversed by Tolbutamide, indicating the involvement of K-ATP channels. C. Voltage clamp recording (VHold=-60mV) of a typical heat inhibited PV neuron in the presence of TTX. Ramping of temperature to 40°C results in an outward current (130.7±38.1pA; n=4; P<0.05)). Gaussian fits (right) of averaged holding current frequency distributions in control (green) and at the peak of temperature response (red). D. Averaged voltage clamp ramps (n=4) acquired in control (green) and at the peak of the temperature response (red). Input resistances were calculated as the inverse of the slope of the linear fit and used to calculate heat induced current with reversal at -85mV typical of the activation of a potassium current. E. Colocalization of AHA pv+ neurons (green) with temperature-activated transient receptor potential (TRP, red) channels TRPV4 (15 of 27 pv+ cells were positive for TRPV4) and TRPM8 (23 of 30 pv+ cells were positive for TRPM8). F. Current clamp recording of a TRH inhibited neuron with an increase in inhibitory post synaptic potentials (IPSP). G. 1. Control trace from the recording in h and held below threshold to show synaptic events. 2. TRH causes pronounce increase in IPSPs.

# Supplementary Figure 3

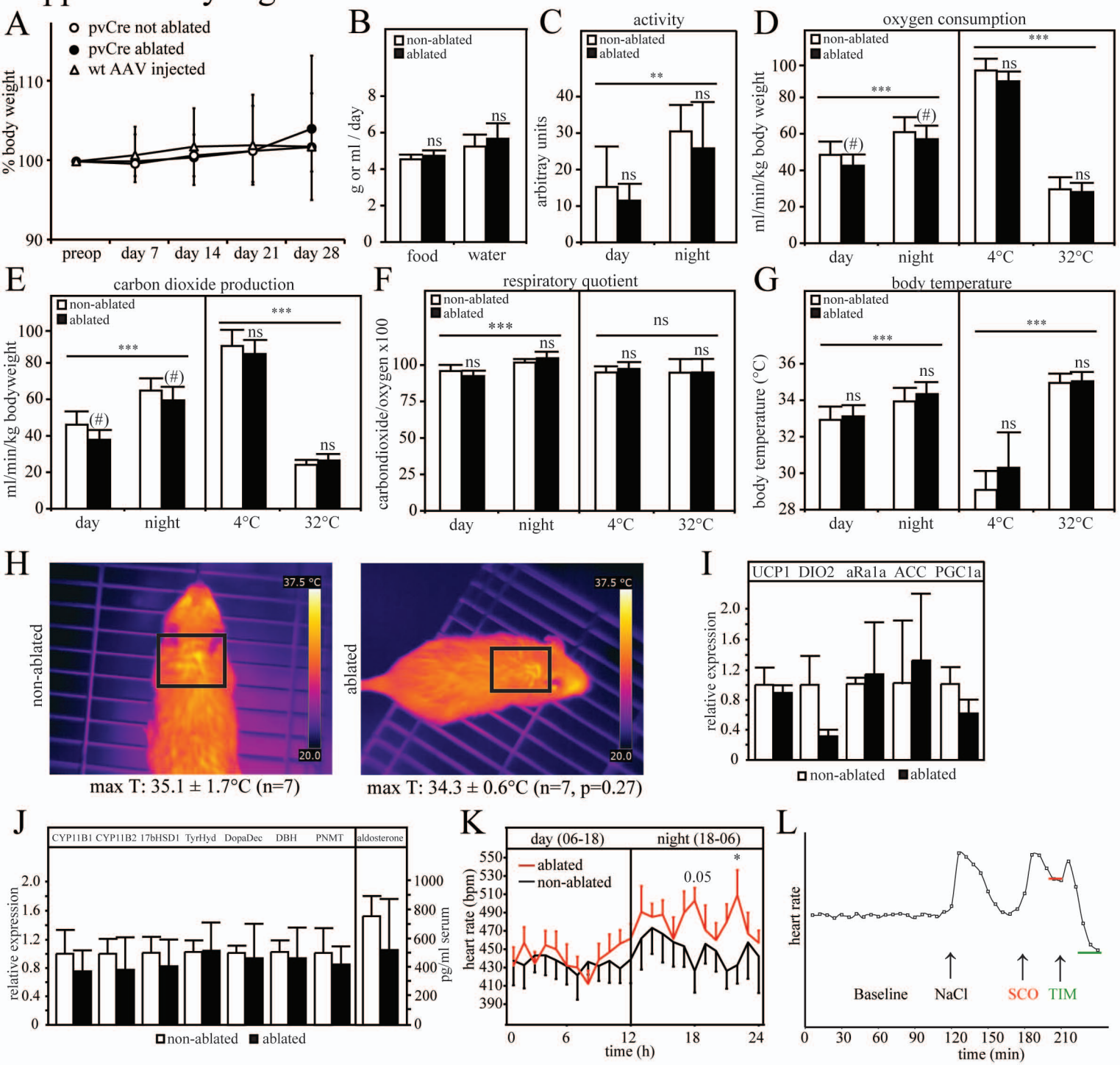


Supplementary Figure 3: A. Weight of AAV injected wildtype, non ablated and ablated pvCre mice before (preop) and after stereotaxic injection. B. Food and water intake in these animals (n.s:not significant). C. Movement activity in these animals at day and night, (**: $p<0.01$ for day versus night, 2-way ANOVA). D/E. Oxygen consumption and carbon dioxide production in these animals at day and night, as well as 4°C and 32°C environmental temperature (***: $p<0.001$ for day versus night, (#): $p<0.05$ for ablation with non-significant posthoc test, 2-way ANOVA. F. Respiratory quotient in these animals at day and night, as well as 4°C and 32°C environmental temperature (***: $p<0.001$ for day versus night, 2-way ANOVA). G. Body temperature in these animals at day and night, or 4°C and 32°C respectively (***: $p<0.001$ for day versus night, 2-way ANOVA). The presented temperature is below core body temperature, as it is recorded with a radiotransmitter in the abdomen close to the skin. H.Infrared thermograph pictures of these animals showing no brown adipose tissue activation. I. Realtime PCR analysis of brown fat mRNA levels in these animals. UCP1: uncoupling protein 1; DIO2: deiodinase type II; aRa1a: adrenergic receptor α1a; ACC: acetyl CoA carboxylase; PGC1a: PPARg coactivator 1 alpha. J. Realtime PCR analysis of adrenal mRNA levels and aldosterone serum levels in mice with reduced number of pv+ cells in the AHA. All differences are not significant ($p>0.05$). CYP11B1/2: cytochrome P450 mitochondrial 11B1 or B2 (steroid 11β hydroxylase), 17bHSD1: 17β-hydroxysteroid dehydrogenase, TyrHyd: tyrosine hydroxylase, DopaDec: DOPA decarboxylase, DBH: dopamine-β-hydroxylase, PNMT: phenyl-N-methyltransferase. K. Heart rate in these animals at day and night time kept at room temperature (n=6 per group, *:$p<0.05$, ANOVA for repeated measurements). L. Schematic overview of the pharmacological autonomic deinnervation experiment in an animal equipped with an implantable radiotransmitter, indicating the time points of injection of saline (NaCl), parasympathetic antagonist scopolamine (SCO) and the sympathetic adrenergic blocker timolol (TIM) with arrows. All values in this supplementary figure are mean ± standard deviation.

Supplementary Table 1: Primer Sequences Realtime PCR

| **Gene Name** | **frw (5'-3')** | **rev (5'-3')** |
|---|---|---|
| 17β-Hydroxysteroid Dehydrogenase | TCCTGGCTCCTTGGAGATACT | TCTAGCGGCCCAAACAAGC |
| Angiotensin Converting Enzyme | AGGTTGGGCTACTCCAGGAC | GGTGAGTTGTTGTCTGGCTTC |
| Angiotensinogen | TCCCGACTAGATGGACACAAG | AGAGGGCAGGGGTAAAGAGAG |
| Calbindin | TCTGGCTTCATTTCGACGCTG | ACAAAGGATTTCATTTCCGGTGA |
| Calretinin | AGTACACCCAGACCATACTACG | GGCCAAGGACATGACACTCTT |
| Cytochrome P450 Subfamily 11B1 | AACCCAAATGTTCTGTCACCAA | CAAAGTCCCTTGCTATCCCATC |
| Cytochrome P450 Subfamily 11B2 | TGGCTGAAGATGATACAGATCCT | CACTGTGCCTGAAAATGGGC |
| Dopa Decarboxylase | GACTACAGGCACTGGCAGAT | CTGGCGTACCAGTGACTCAA |
| Dopamine β Hydroxylase | TGGACCCCGAAGGGATTTTAG | CCATCTCTCCTCGATCTGACA |
| Parvalbumin | ATCAAGAAGGCGATAGGAGCC | GGCCAGAAGCGTCTTTGTT |
| Phenyl N-Methyl Transferase | CAGACCTGAAGCACGCTACAG | TAGTTGTTGCGGAGATAGGCG |
| Renin | ACGGGTCCGACTTCACCAT | TGCCTAGAACACCGTCAAACT |
| Tyrosine Hydroxylase | GCTGGAGGATGTGTCTCACT | GAGGAGGCATGACGGATGTA |